

AD-A046 639

CINCINNATI UNIV OHIO
AERODYNAMIC EFFECTS ON EROSION IN TURBOMACHINERY, (U)
1977 W TABAKOFF, A HAMED

F/G 21/5

UNCLASSIFIED

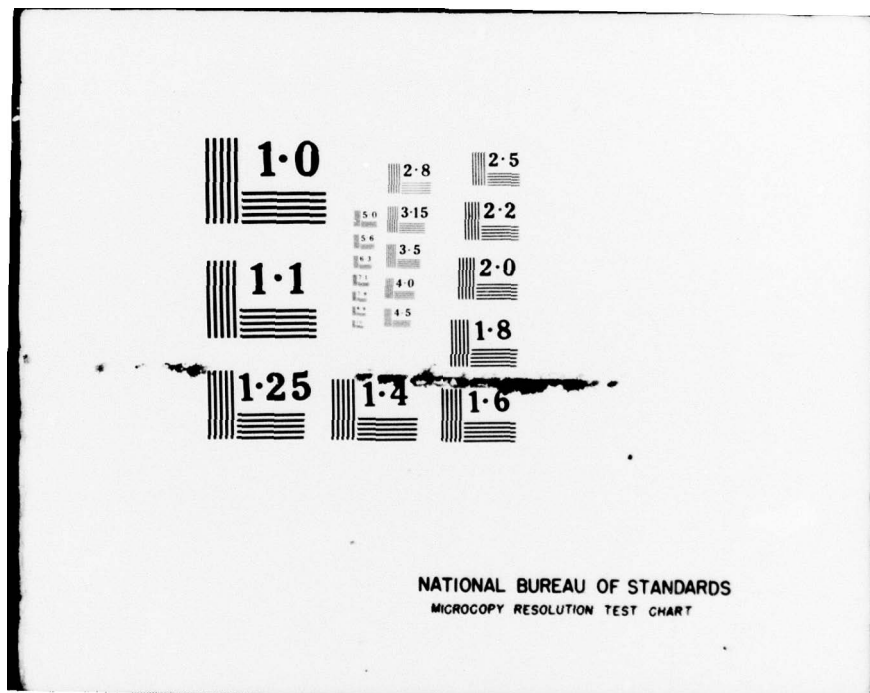
1 OF 1
ADA
046639



ARO-13653.1-E

NL

END
DATE
FILMED
12-77
DDC



(8) (9) REPORT DOCUMENTATION PAGE		READ INSTRUCTIONS BEFORE COMPLETING FORM
1. REPORT NUMBER ARO 13653.1-E	2. GOVT ACCESSION NO.	3. RECIPIENT'S CATALOG NUMBER
4. TITLE (AND SUBTITLE) AERODYNAMIC EFFECTS ON EROSION IN TURBOMACHINERY		5. TYPE OF REPORT & PERIOD COVERED Reprint
6. PERFORMING ORG. REPORT NUMBER 10	7. AUTHOR(s) W. Tabakoff A. Hamed	
8. CONTRACT OR GRANT NUMBER(s) DAAG29-76-G-0229 E(18)-2465		9. PERFORMING ORGANIZATION NAME AND ADDRESS University of Cincinnati
10. CONTROLLING OFFICE NAME AND ADDRESS U. S. Army Research Office Post Office Box 12211 Research Triangle Park NC 27700		11. REPORT DATE 11 1977
12. MONITORING AGENCY NAME & ADDRESS (if different from Controlling Office)		13. NUMBER OF PAGES 7 129p.
14. DISTRIBUTION STATEMENT (of this Report)		15. SECURITY CLASS. (of this report) Unclassified
16. DISTRIBUTION STATEMENT (of the abstract entered in Block 20, if different from Report)		15a. DECLASSIFICATION/DOWNGRADING SCHEDULE D D C NOV 21 1977
17. SUPPLEMENTARY NOTES The findings in this report are not to be construed as an official Department of the Army position, unless so designated by other authorized documents.		
18. KEY WORDS (Continue on reverse side if necessary and identify by block number)		
19. ABSTRACT A unique erosion test facility was designed such that the aerodynamic effects are an integral part of the test parameters. The alloys studied in this investigation are 2024 aluminum, 410 stainless steel and 6A1-4V titanium. High speed movies were used to examine and determine the impact and rebound characteristics of the solid particles. The effects of particle velocity and impact angle were found to be statistical in nature. The statistical distributions of these impact parameters were determined experimentally. The rebound data was then related to the erosion damage incurred. In addition, the effect of temperature on the erosion of the alloys was also studied.		



1977 Tokyo
Joint Gas Turbine Congress

Aerodynamic Effects on Erosion in Turbomachinery

W. Tabakoff

University of Cincinnati, Cincinnati, Ohio

A. Hamed

University of Cincinnati, Cincinnati, Ohio

A unique erosion test facility was designed such that the aerodynamic effects are an integral part of the test parameters. The alloys studied in this investigation are 2024 aluminum, 410 stainless steel and 6A1-4V titanium. High speed movies were used to examine and determine the impact and rebound characteristics of the solid particles. The effects of particle velocity and impact angle were found to be statistical in nature. The statistical distributions of these impact parameters were determined experimentally. The rebound data was then related to the erosion damage incurred. In addition, the effect of temperature on the erosion of the alloys was also studied.

Contributed by Gas Turbine Society of Japan for presentation at 1977 Tokyo Joint Gas Turbine Congress held in Tokyo, Japan on May 22nd to 27th, 1977 under the co-sponsorship of Gas Turbine Society of Japan, the Japan Society of Mechanical Engineers and the American Society of Mechanical Engineers. Manuscript received at GTSJ on Oct. 15th, 1976.

AERODYNAMIC EFFECTS ON EROSION IN TURBOMACHINERY

W. Tabakoff¹ and A. Hamed²

ABSTRACT

A unique erosion test facility was designed such that the aerodynamic effects are an integral part of the test parameters. The alloys studied in this investigation are 2024 aluminum, 410 stainless steel and 6Al-4V titanium. High speed movies were used to examine and determine the impact and rebound characteristics of the solid particles. The effects of particle velocity and impact angle were found to be statistical in nature. The statistical distributions of these impact parameters were determined experimentally. The rebound data was then related to the erosion damage incurred. In addition, the effect of temperature on the erosion of the alloys was also studied.

NOMENCLATURE

D	Particle diameter.
IGV	Inlet guide vane.
K_1, K_3, K_{12}	Material constants.
Re	Reynolds number.
V	Particle velocity.
β	Relative angle between particle path and specimen surface.
ϵ	Erosion per unit mass of impacting particles.
μ	Microns.
σ	Standard deviation of a normal distribution.

Subscripts

1	Conditions of the particle approaching the target.
2	Conditions of the particle rebounding from the target.
N	Normal component.
T	Tangential component.

¹ University of Cincinnati, Cincinnati, Ohio.

² University of Cincinnati, Cincinnati, Ohio.

Contributed by Gas Turbine Society of Japan for presentation at 1977 Tokyo Joint Gas Turbine Congress held in Tokyo, Japan on May 22nd to 27th, 1977 under the co-sponsorship of Gas Turbine Society of Japan, the Japan Society of Mechanical Engineers and the American Society of Mechanical Engineers. Manuscript received at GT SJ on Oct. 15th, 1976.

INTRODUCTION

In many industrial and military applications the erosive action of high speed particles results in serious problems. Erosion has been pointed out as a problem in as diverse areas as aero gas turbines, rocket nozzles, coal fired boiler systems, and catalytic cracking equipment. Recent interest in this old problem coincides with increased usage of gas turbines in dusty terrains. If erosion can be incorporated as an engine design parameter, an erosion tolerant engine can possibly be produced.

Historically, erosion has been studied as a two part problem. The first part involves the determination of the number, direction and velocity of the particles striking the surface which is naturally affected by the flow conditions. With such information available, the second part of the problem involves the calculation of the surface material removed. These two problems have always been considered to be independent of one another, however, in the complicated flow fields existing within rotating machinery, it is questionable whether this assumption is valid.

The theoretical studies concerning erosion are predominantly empirical. They involve basic assumptions as to the process governing material removal. Finnie [1] and Smeltzer, et al. [2] have conducted a theoretical analysis of the erosion of ductile materials. In more recent investigations [3-5] further insight into the actual mechanism of erosion has been obtained by examining the target surface at high magnification using metallographic techniques and electron microscopy.

In 1959, Finnie [3] described a sand blasting erosion test facility. This facility, in which a small jet of particle laden air was impacted on a stationary specimen. By far the majority of erosion research has been conducted using this facility or modifications of it.

EXPERIMENTAL EQUIPMENT

As mentioned previously, the test facilities designed thus far, did not simulate the aerodynamic effect of the flow field over

the erosion specimen. This can particularly be a very important factor in turbomachine erosion, where the flow is constantly turned by rotating and stationary cascades. Two erosion test facilities were therefore built during the course of this study. The first wind tunnel with stationary specimen was designed to obtain basic erosion data and particle impact and rebound characteristics. Another unique test facility was then designed to simulate and measure the erosion of turbomachine blades.

Stationary Specimen Test Facility

In designing this wind tunnel, controlling the various erosion parameters such as fluid velocity, particle velocity, particle flow rate and particle size was of primary importance. The effects of variations in the specimen size, as well as the angle of incidence between the abrasive particles and the surface of the specimen were also investigated. Besides obtaining erosion data in an aerodynamic environment, this test facility was also used to determine the particle impact and rebound characteristics using high speed photography.

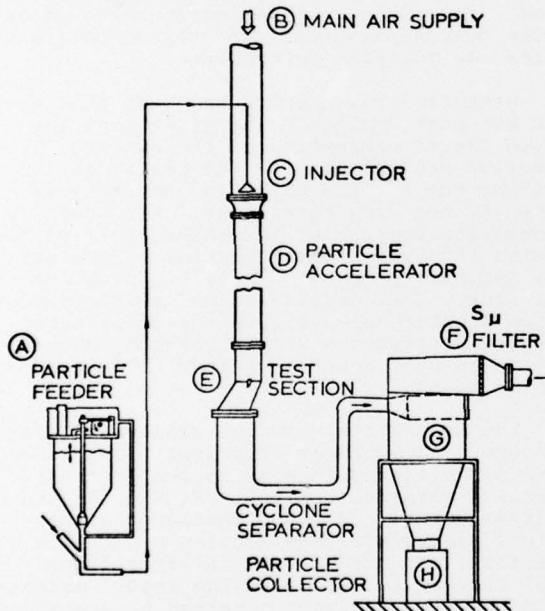


Fig. 1 Erosion test facility

Figure 1 is a schematic of the apparatus developed for that purpose. As depicted in this illustration, the equipment functions as follows: A measured amount of abrasive grit of a given consistency is placed into the particle feeder, A. The particles are fed into a secondary air source and blown up to the particle injector, C, where it mixes with the main air supply, B. The particles are then accelerated by the high velocity air in a constant area duct, D, and impact the specimen in test section, E. The test dust is then separated from the air by a cyclone

separator, G, and collected in the container, H. The test air is further filtered through a commercial 5 μ filter, F.

Since the particles are accelerated in the constant area duct by the aerodynamic drag forces, their velocity before impacting the specimen would depend upon the air velocity, the particle size and the length of the acceleration section, D. Figure 2 gives an illustration of the dynamics of relatively large, 200 μ , and relatively small, 20 μ , particles in two flow velocity fields 400 and 1000 ft/sec. From this figure it can be seen that the particle's final velocity is an exponential function of the tunnel length.

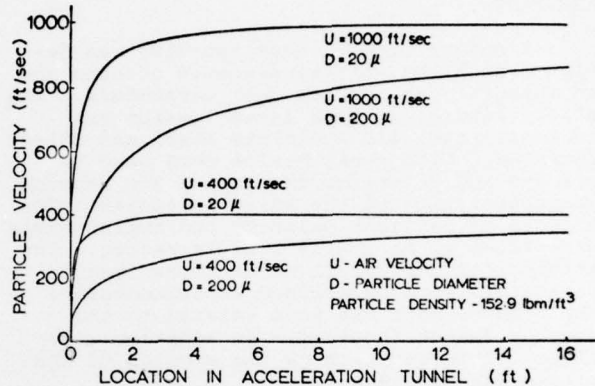


Fig. 2 Particle dynamics in the tunnel

Figure 3 shows that, as expected, a longer tunnel will result in higher particle velocities, and that particle size would have a diminishing effect on particle velocity in longer tunnels. Based on these findings, a tunnel length of 12 feet and a 1 x 3 inch rectangular cross section was used in obtaining the rest of the experimental data.

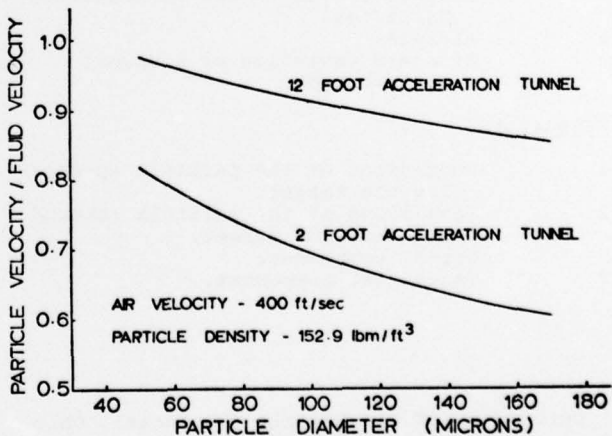


Fig. 3 Effect of tunnel length

From Figure 1 it can be seen that the tunnel geometry is uninterrupted from the acceleration tunnel into the test section.

In this manner the particle laden air is channeled over the specimen and the aerodynamics of the fluid passing over the blade at the given angle of attack are preserved. In order to minimize the tunnel blockage, 3 sized specimens were used. At angles of attack of 0 to 20 degrees a one inch wide specimen was used, from 20 to 45 degrees, a half inch wide specimen was used and for the large angles of attack of 45 to 90 degrees, a quarter inch wide specimen was used.

The test section has an insert through which high-speed photography and streak photographs can be taken of the high-speed sand particles. In this manner the velocity of the approaching sand particle was obtained and compared to the theoretical predictions.

Rotating Specimen Erosion Facility

This unique facility was designed such that the erosion of stationary and rotational turbomachine blades can be measured. Figure 4 shows a schematic of the facility in which a measured amount of abrasive grit of a given consistency is placed in the particle feeder at A. The particle feeder used with this facility is the same as was described earlier for use in the stationary facility. The particles are fed into a secondary source, blown up to the system inlet and injected at B. The particles are then accelerated by the air that is being sucked through the inlet section, C, to the test section, D. The spent dust is then collected in a filter bag, E.

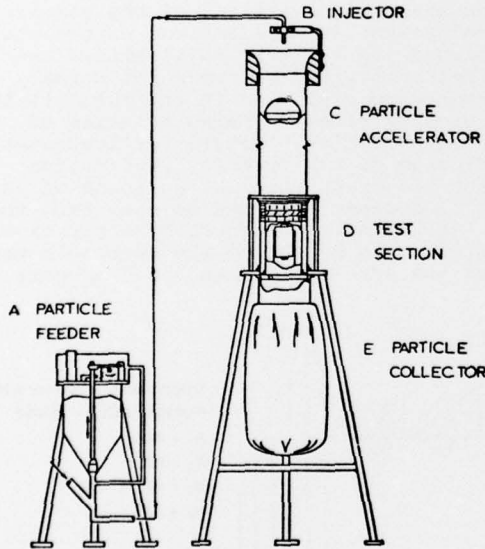


Fig. 4 Rotating machinery erosion facility

The test section consists of specimen blades simulating inlet guide vanes, rotor blades, and straightening vanes. The rotor is driven by a one-half horsepower, 10,000 RPM variable speed motor. The inlet guide vane, rotor and straightening vane blades are designed such that they are easily removable so that they may be weighed and thus erosion measured.

Photographic Method for Determining Particle Velocities

In this research it was decided to use high-speed photography as a means of particle flow visualization. The development of this technique was difficult in that no literature could be found concerning the problem and a certain amount of trial and error development work was necessary. However, the method was chosen as it allowed a large number of data points to be taken at the same time, thus keeping the flow conditions unchanged and hence an accurate assessment of the particle environment can be made.

The camera used to photograph the particles was a 16mm Hycam camera with a one-half framer, enabling 22,000 half frames per second to be produced at top speed. The pictures were taken on 400 foot rolls of 4x Reversal Kodak high speed film using two Sylvania FF-33 flood flash lamps as a source of light. The particles were recorded on the film as a result of back-scatter of light off of them, thus it was important that a very dark, nonreflecting background be used. The particle velocities were obtained by comparing the distance traveled by the particle in two successive frames to this reference distance.

DEVELOPMENT OF PARTICLE REBOUND CORRELATIONS

The erosion of metals impacted by small dust particles as well as the rebound dynamics of these particles can only be described in a statistical sense. This becomes obvious when one examines the number of geometric situations that might be involved at impact. After a given incubation period, the target material will become pitted with craters and in fact after a slightly longer period, a regular ripple pattern may form on the eroded surface. Thus the local impact angle between the small particle and the eroded surface may deviate considerably from the geometric average. Further, the particles themselves are irregular crystalline in shape with several sharp corners. Therefore as the particle approaches the specimen, the orientation of the particle is, for the most part, random.

The restitution coefficient or restitution ratio is a measure of the kinetic energy exchange between two objects upon impact. Since erosion is a function of the energy exchange between the erodent particle and the material impacted, it was felt that the restitution ratio will give a good indication of the behavior of the particle-material interaction. This investigation was limited to ductile target materials only. In addition the contaminant particles were chosen to be much harder than the target material. Therefore, the restitution ratio will be a measure of target distortion rather than distortion of the erosive particle.

The ratio of the particle velocity before and after impact (V_2/V_1) is plotted against the angle of attack (β_1) in Figure 5. Since the statistical distributions are of importance, the shape of these distributions are

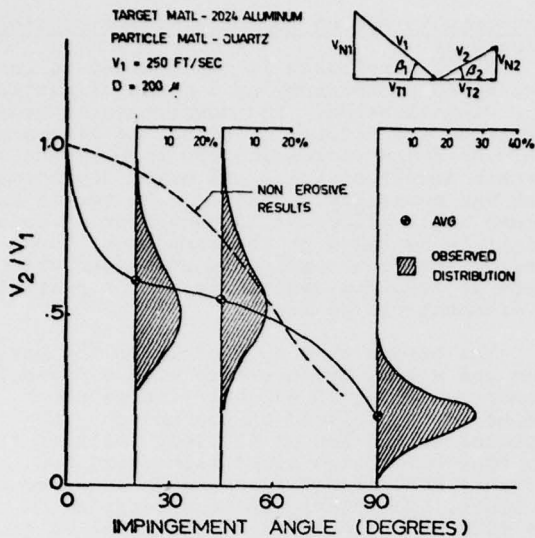


Fig. 5 Influence of impact angle of particle velocity restitution ratio

cross plotted on the figure. The spread in this data indicates the variable condition of the surfaces and the orientation of the particle at impact. Further, the data obtained by Hussein [6] for nonerosive particles are plotted in the same figure for comparison.

Grant, Ball and Tabakoff [7] were the first to thoroughly investigate the rebound characteristics of high-speed eroding particles. The study was carried out on annealed 2024 aluminum alloy. The data was described using histograms to illustrate its statistical distribution. As with Hussein and Tabakoff [8] curve fit equations were also obtained for the data. It was concluded from this investigation that the restitution ratio (V_2/V_1), which is directly related to the kinetic energy lost during impact, does not give sufficient information in regard to erosion. With this in mind, the restitution ratio was broken down into a normal velocity restitution ratio, V_{N2}/V_{N1} , (the normal component of the particle velocity after impact/the normal component of the particle velocity before impact), and a tangential velocity restitution ratio, V_{T2}/V_{T1} , (the tangential component of the particle velocity after impact/the tangential component of the particle velocity before impact). It was found that the normal velocity restitution ratio does not significantly contribute to ductile erosion. Most probably the kinetic energy is dissipated by plastic deformation of the target material without significant material removal. When the tangential velocity restitution ratio was investigated, it was found that the maximum erosion of 2024 aluminum which was observed at 20 degrees angle of attack [7], coincides with the minimum value of V_{T2}/V_{T1} . The equations predicting the behavior of the various restitution ratio parameters were found to be :

$$V_{T2}/V_{T1} = 1.0 - 2.03\beta_1 + 3.32\beta_1^2 - 2.24\beta_1^3 - 0.472\beta_1^4 \quad (1)$$

$$\beta_2/\beta_1 = 1.0 + 0.409\beta_1 - 2.52\beta_1^2 + 2.19\beta_1^3 - 0.531\beta_1^4 \quad (2)$$

$$V_{N2}/V_{N1} = 0.993 - 1.76\beta_1 + 1.56\beta_1^2 - 0.49\beta_1^3 \quad (3)$$

$$V_{T2}/V_{T1} = 0.988 - 1.66\beta_1 + 2.11\beta_1^2 - 0.67\beta_1^3 \quad (4)$$

where β_1 is the incidence angle in radians.

Since the data is of a statistical nature the equations for the standard deviation of the normal and tangential velocity restitution ratios were also obtained, so that the effect of impact angle on the statistical behavior of the parameters could be examined. The equations for the standard deviation, σ , of the normal distributions are as follows:

$$\sigma(V_{T2}/V_{T1}) = 0.005 + 0.62\beta_1 - 0.535\beta_1^2 + 0.089\beta_1^3 \quad (5)$$

$$\sigma(V_{N2}/V_{N1}) = 2.15\beta_1 - 5.02\beta_1^2 + 4.05\beta_1^3 - 1.085\beta_1^4 \quad (6)$$

The standard deviations of the restitution coefficient (V_2/V_1) and the directional coefficients (β_2/β_1) were not examined because their distributions were not normal. Histograms were also used in the presentation of the erosive rebound characteristics of high-speed particles. Figure 6 illustrates the histogram of the velocity restitution ratio for stainless steel at an angle of attack of 15 degrees. As can be seen from this figure, the data is presented by a series of rectangles. The height of the rectangle represents the number of times, or frequency of

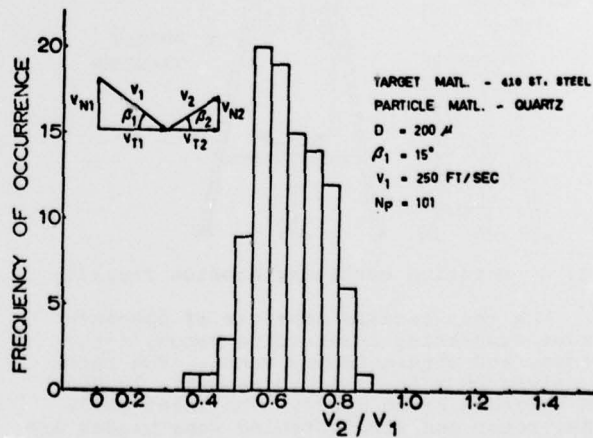


Fig. 6 Erosive particle velocity restitution ratio distribution

occurrence that the velocity restitution ratio was found to be between the limits designated by the scale at the base of the rectangle. The spread in the data indicates that the condition of the material surface and the orientation of the particle at impact changes.

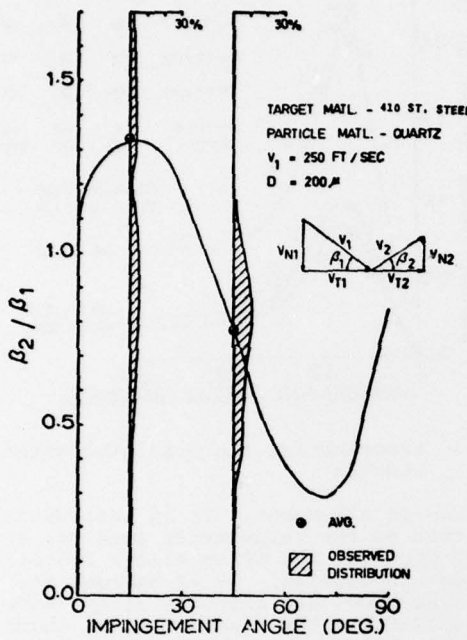


Fig. 7 Influence of impact angle on particle directional coefficient

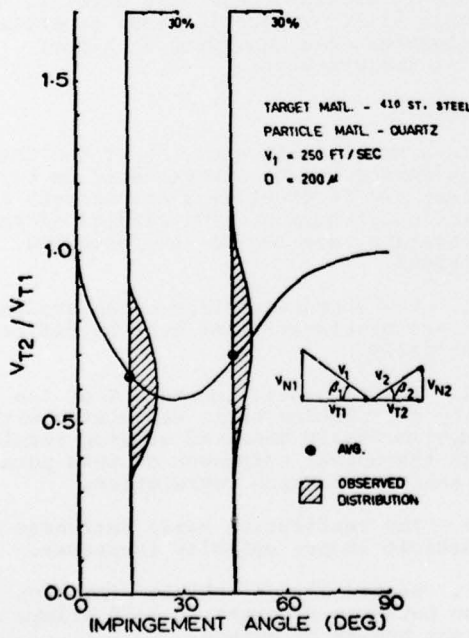


Fig. 8 Influence of impact angle on tangential velocity restitution ratio

Figure 7 shows the data summarized for the directional coefficient distribution of stainless steel for 15 and 45 degrees.

The ratio of the tangential component of velocity v_{T2}/v_{T1} for stainless steel at angles of attack of 15 and 45 degrees is shown in Figure 8, where the tangential restitution ratio at 90 degrees was assumed to be unity. From the experimental findings a least square, polynomial curve fit was obtained for the restitution parameter which may be expressed by the following equations:

$$v_2/v_1 = 1.0 - 2.0586\beta_1 + 3.0748\beta_1^2 - 1.3184\beta_1^3 \quad (7)$$

$$\beta_2/\beta_1 = 1.0 + 2.6067\beta_1 - 5.7083\beta_1^2 + 2.5358\beta_1^3 \quad (8)$$

$$v_{N2}/v_{N1} = 1.0 - 0.4159\beta_1 - 0.4994\beta_1^2 + 0.2928\beta_1^3 \quad (9)$$

$$v_{T2}/v_{T1} = 1.0 - 2.12\beta_1 + 3.0775\beta_1^2 - 1.18\beta_1^3 \quad (10)$$

Equations for the standard deviation of the normal and tangential velocity restitution ratios were obtained and are given by:

$$\sigma(v_{T2}/v_{T1}) = 0.4523\beta_1 - 0.2876\beta_1^2 - 0.0309\beta_1^3 + 0.195\beta_1^4 \quad (11)$$

$$\sigma(v_{N2}/v_{N1}) = 2.5104\beta_1 - 3.1693\beta_1^2 - 0.2755\beta_1^3 + 0.8273\beta_1^4 \quad (12)$$

Similar experiments were performed with the titanium alloy.

DISCUSSION OF EXPERIMENTAL RESULTS

The tangential restitution ratio was also found to be very susceptible to the magnitude of the approach velocity. This fact is very significant in erosion prediction which is mostly affected by that parameter. According to the experimental data, the tangential restitution ratio, R_T , was found to be linearly proportional to the normal component of the impact velocity. An expression of this relationship for 2024 aluminum is:

$$R_T = 1.0 - 0.0016 v_1 \sin(\beta_1) \quad (13)$$

The tangential restitution ratio for 410 stainless steel is expressed as:

$$R_T = 1.0 - 0.0017 v_1 \sin \beta_1 \quad (14)$$

and the tangential restitution ratio for 6Al-4V titanium was found to be:

$$R_T = 1.0 - 0.0016 V_1 \sin \beta_1 \quad (15)$$

These expressions were used in the erosion equations developed by Grant and Tabakoff [10] to predict the erosion behavior of the different target materials.

Prediction of Ductile Alloys Erosion

The equation for predicting the erosion, ϵ , of the specimen material can be expressed as follows:

$$\epsilon = K_1 f(\beta_1) V_1^2 \cos^2 \beta_2 [1 - R_T^2] + f(V_{in}) \quad (16)$$

where

$$f(\beta_1) = 1 + CK(K_{12}) \sin^2 \beta_0 \quad (17)$$

$$f(V_{in}) = K_3 (V_1 \sin \beta_1)^4 \quad (18)$$

β_0 = angle of attack where maximum erosion occurs.

The empirical constants for quartz impacting on aluminum alloy are:

$$K_1 = 3.67 \times 10^{-6}, \quad K_{12} = 0.585$$

$$K_3 = 6.0 \times 10^{-12}$$

$$CK = 1 \quad \text{for } \beta_1 \leq 20$$

$$CK = 0 \quad \text{for } \beta_1 > 0$$

The previously reported restitution ratios were used in equation (16) to predict the erosion of the different target materials which was found to agree with the experimentally measured values. The experimental results for alumina (Al_2O_3) impacting on aluminum alloy in the stationary specimen test facility were found to be similar but slightly lower than those obtained using conventional erosion test facilities.

Figure 9 illustrates the erosion results for 2024 aluminum alloy at different particle velocities. Inspection of the figure shows that the maximum erosion occurs at an angle of approximately 20 degrees. As the angle of attack increases from this value the erosion reduces to a residual value at 90 degrees. The solid curves show the values computed using equation (16).

Effect of Material Temperature on Erosion

To the present date no sufficient research is reported regarding the effect of material temperature on erosion. For this purpose, erosion studies of heated alloys in the stationary specimen facility were carried out. Three different alloys at three angles of attack ($\alpha = 20, 60$ and 90 degrees) were investigated. The alloys tested were 2024 aluminum, 410 stainless steel and 6Al-4V titanium. The diameter of the particles used was 138 microns and the particles velocity was 410 ft/sec. The material temperature was varied between room temperature and 400 F. The experimental results are shown in Figure 10 for the three alloys. The linear dependence between erosion and temperature can be

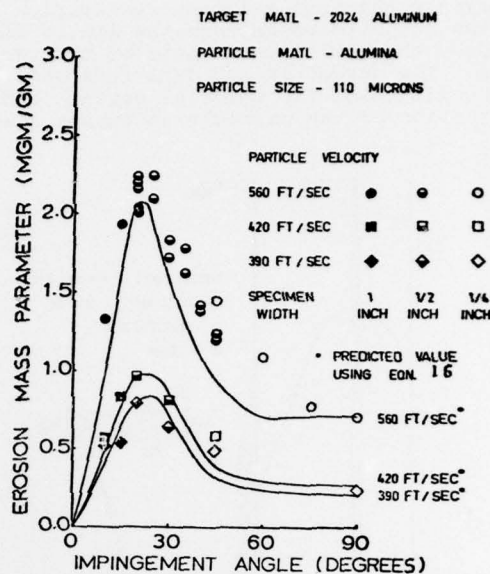


Fig. 9 Experimental and predicted erosion results

observed in all cases. It is interesting to note that as the temperature goes up, at $\alpha = 20$ degrees, the three alloys exhibit a decrease in erosion. At 60 degrees the stainless steel and titanium alloys show a decrease, while the aluminum alloy shows an increase in erosion with increase temperatures. At 90 degrees the titanium alloy shows an erosion decrease with increasing temperature, while the other two show an increase in erosion. For more details, see Reference [11]. Presently these experimental investigations are continued at higher material temperatures.

CONCLUSIONS

In general, this study shows how the erosion damage can be investigated in turbo-machinery and it provides a new insight into the erosion phenomena. The results of this investigation have led to the following conclusions.

1. The characteristics of an eroding system are problematic and must be defined statistically.

2. The tangential component of the velocity restitution ratio correlates with the experimentally observed erosion results, whereas the normal component of this parameter exhibits no such correlation.

3. The restitution ratio decreases as the particle impact velocity increases.

4. Heated alloys exhibit different erosion patterns compared to cold alloys at different angles of attack.

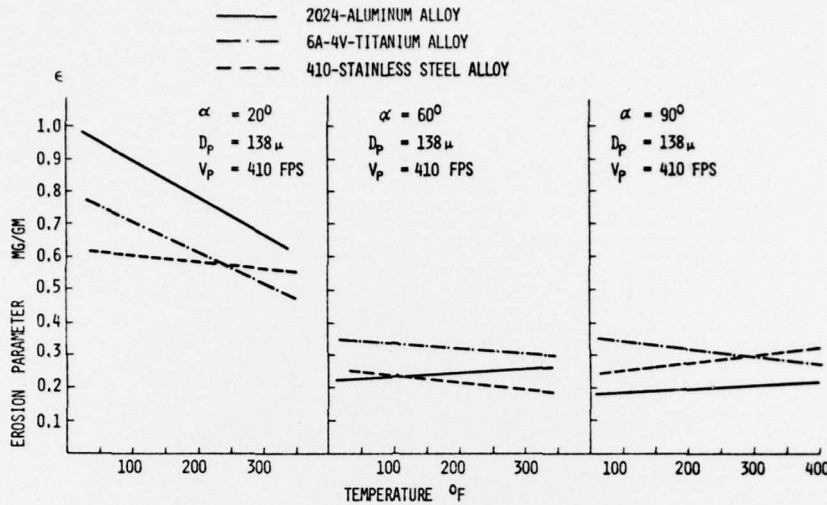


Fig. 10 Effect of temperature on erosion for three alloys

ACKNOWLEDGEMENT

This work was partially sponsored by U.S. Army Research Office - Durham under Contract No. DAAG-29-76-G-0229 and partially by ERDA Contract No. E(49-18)-2465.

REFERENCES

- [1] Finnie, I., Wolak, J. and Kabil, Y., "Erosion of Metals by Solid Particles," *Journal of Materials*, Vol. 2, No. 3, September 1967, pp. 682-700.
- [2] Smeltzer, C.E., Gulden, M.E., McElmury, S.S. and Compton, W.A., "Mechanisms of Sand and Dust Erosion in Gas Turbine Engines," *USAALVLABS Technical Report*, August 1970.
- [3] Finnie, I., "An Experimental Study on Erosion," *Proceedings of the Society for Experimental Stress Analysis*, Vol. XVII, No. 2, pp. 65-70.
- [4] Smeltzer, C.E., Gulden, M.E. and Compton, W.A., "Mechanisms of Metal Removal by Impacting Dust Particles," *Journal of Basic Engineering*, September 1970, pp. 639-654.
- [5] Head, W.J. and Harr, M.E., "The Development of a Model to Predict the Erosion of Materials by Natural Contaminants," *Wear*, Vol. 15, 1970, pp. 1-46.

[6] Hussein, M.F., "The Dynamic Characteristics of Solid Particles in Particulated Flow in Rotating Machinery," *Ph.D. Thesis*, University of Cincinnati, 1972.

[7] Grant, G., Ball, R. and Tabakoff, W., "An Experimental Study of the Erosion Rebound Characteristics of High-Speed Particles Impacting a Stationary Specimen," *Dept. of Aero. Engg. Technical Report 33-36*, May 1970, AD-760578.

[8] Hussein, M.F. and Tabakoff, W., "Calculation of Particle Trajectories in a Stationary Two-Dimensional Cascade," *Dept. of Aero. Engg. Technical Report No. 72-27*, University of Cincinnati, 1972, AD-764267.

[9] Ball, R. and Tabakoff, W., "An Experimental Investigation of the Particle Dynamics of Quartz Sand Impacting 6Al-4V Titanium in an Erosive Environment," *Dept. of Aero. Engg. Technical Report No. 74-43*, University of Cincinnati, 1974.

[10] Grant, G. and Tabakoff, W., "Erosion Prediction in Turbomachinery Due to Environmental Solid Particles," *Journal of Aircraft*, Vol. 12, May 1975, pp. 471-478.

[11] Gat, N., "The Effect of Temperature on Erosion," *M.S. Thesis*, Dept. of Aero. Engg., University of Cincinnati, 1975.

ACCESSION for	
NTIS	White Section <input checked="" type="checkbox"/>
DDC	Buff Section <input type="checkbox"/>
UNANNOUNCED	
JUSTIFICATION	
BY	
DISTRIBUTION/AVAILABILITY CODES	
Disc.	SP. CIAL
A	